31 Mar 2001, 8:00 am - 9:30 am

Earthquake Resistance of New Type Viaduct Structure

Eiji Wakita
National Gunma College of Technology, Japan

Masayoshi Sato
National Research Institute for Earth Science and Disaster Prevention, Japan

Takashi Tazoh
Shimizu Corporation, Japan

Proceedings: Fourth International Conference on Recent Advances in Geotechnical Earthquake Engineering and Soil Dynamics and Symposium in Honor of Professor W.D. Liam Finn
San Diego, California, March 26-31, 2001

EARTHQUAKE RESISTANCE OF NEW TYPE VIADUCT STRUCTURE

Eiji Wakita
National Gunma College of Technology,
580, Toriba-machi, Maebashi,
Gunma, 371-0845, JAPAN

Masayoshi Sato
National Research Institute for Earth Science and Disaster Prevention,
Tukuba, 305-0006, JAPAN

Takashi Tazoh
Institute of Technology,
Shimizu Corporation,
Tokyo, JAPAN

ABSTRACT

An experiment and a numerical analysis were carried out in order to examine the earthquake resistance of a new type viaduct structure. The experiment was a dynamic centrifuge modeling which used the viaduct model of the rates 1/50 of a scale. The 3-dimensional finite element analysis was performed in order to confirm the results of the dynamic centrifuge modeling. At the results, new knowledge was obtained with regard to the viaduct structure.

INTRODUCTION

The Kobe earthquake occurred big damages in many railroad viaducts in 1996 in Japan. It becomes the important issue to secure the earthquake resistance of the viaducts in Japan. The adoption of the CFT as the pillar of the viaduct is a good way of the improvement of the earthquake resistance. The CFT is an abbreviated word of the Concrete Filled steel Tube (Shioya et al., 1999). The feature of the CFT is the big toughness and the high earthquake resistance that is brought by filling up with concrete within a steel pipe. Furthermore, it is conventionally common to use the connection beam (*Fig. 1*) as the structure of the viaduct. However, removing the connection beam can form a new type viaduct structure. If it possible to omit the connection beam, the construction of viaduct can be more economically attained by the short time for the completion. The experiment and the numerical analysis were carried out to research the behavior at the time of an earthquake. The objects of the experiment and the numerical analysis are the conventional type and the new type of structure mentioned above. In this paper, the rationality and the applicability of them will be examined by using those results.

OUTLINE OF DYNAMIC CENTRIFUGE MODELING

The height of the object viaduct is 11.4m. The lengths of the object viaduct are both 10m in the right-angled and the parallel direction of the viaduct. The pile length is 17m. The ground is consisted with 2 layers. The upper layer is the soft sand layer of 15m and the lower layer is the support layer. The CFT pillar is a steel tube that is filled with concrete and the diameter is 800mm. The pile is steel tube that is filled with concrete and the diameter is 1000mm. The upper beam and the connection beam are the reinforced concrete of $1250mm^{W} \times 900mm^{H}$. The beam weight and train weight are taken into consideration as the loads that contribute to the inertia power at the time of an earthquake.

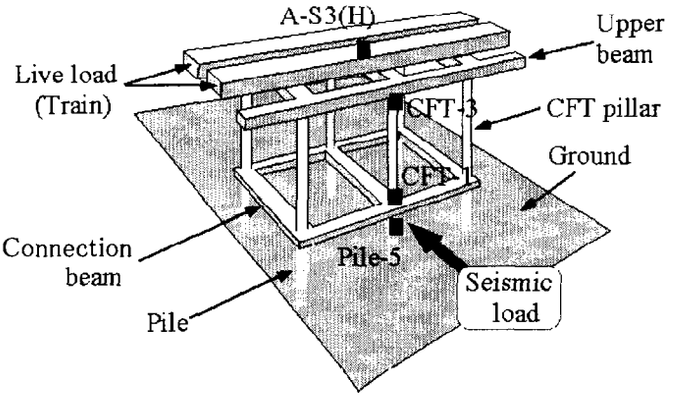

Fig. 1. Viaduct model for experiment and arrangement of instruments (Case equipped with connection beam)

Fig. 1 shows one of the models that were used for the experiment. This case is equipped with the connection beam as shown in the figure. The dynamic centrifuge modeling was executed using a one-fiftieth-scale model of two spans of the viaduct-pile-ground system. The earthquake vibration was given from one direction at the right angle to the viaduct. The pipe that corresponds to the CFT pillar was made with the stainless steel. This pipe was filled with mortar and the diameter was 16 mm. The unit weight of the reinforced concrete and the unit weight of the aluminum are almost a same size, therefore the aluminum was adopted as the material of the upper beam and the connection beam. Lead boards were set on the upper beam. The total weight of the boards was 105N. It corresponds to the train live load. The surface 30cm of the ground was formed with silica sand. The relative density of the ground is 70%.

The support layer was made of poor compounded soil cement. The pile was modeled with a stainless steel pipe of 34cm length and 20mm diameter. The pile head was fixed on the bottom of the CFT pillar. The tip of the pile was inserted into the support layer with the length of the twice of the pile diameter. *Table* 1 shows the similarity rule that was used for the dynamic centrifuge modeling. The experiment results mentioned later will be displayed using the values converted into the real size, for example time and acceleration. There are two cases for the experiment. In this paper, the liquefaction of the ground is not dealt with as the object of the examination. One of them is the Case 1 equipped with the connection beam. Another one is the Case 2 without the connection beam. In order to grasp the response characteristic on the frequency of the viaduct, the following 4 kinds of waves were used as the input waves. (1) El-Cetro seismic wave, 100Gal, (2) 0.6Hz of Sin wave, 50Gal, ten waves, (3) 1.0Hz of Sin wave, 100Gal, ten waves, (4) 2.0Hz of Sin wave, 100Gal, ten waves.

RESULTS OF DYNAMIC CENTRIFUGE MODELING AND ITS CONSIDERATION

To the beginning, in order to grasp the frequency characteristic of the viaduct-pile-ground system, a minute sweep vibration was given of the acceleration 2Gal. *Fig.* 2 shows the transfer function of the top (A-S3) of the viaduct against the ground base (A-GO). A peak is seen near by 0.7Hz at the case equipped with the connection beam. The peak is seen near by 0.6Hz at the case of structure without the connection beam.

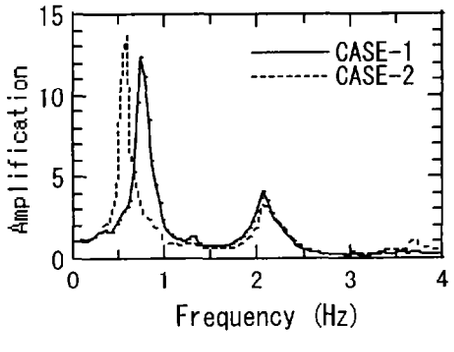

Fig. 2. Transfer function of top of viaduct against ground base

They are the first natural frequencies of the viaducts. The peak that is seen near by 2Hz is the first natural frequency when the strain level is in the early stages of the shear modulus of the soil. *Fig.* 3 shows the time history response of the base input acceleration 0.6Hz-50Gal of Sin wave.

Table 1. Similarity rule for the dynamic centrifuge modeling

Item		Unit	Real Structure	Model for experiment	Scale Ratio
Ground (Upper layer)	Thickness	m	15	0.3	1/N
Ground (Lower layer)	Thickness	m	2.5	0.05	1/N
Pile	Diameter	m	1	0.02	1/N
	Thickness	m	0.0012	0.000024	1/N
	Length	m	17.5	0.35	1/N
	Young Modulus	kN/m^2	2.1E+08	2.1E+08	1
	Bending stiffness	$kN \cdot m^2$	4.82E+05	7.71E-02	$1/N^4$
CFT Pillar	Bending stiffness	$kN \cdot m^2$	4.27E+05	6.83E-02	$1/N^4$
Upper structure	Natural frequency	Hz	0.6	30	N
	Mass	kg	1.94E+06	1.55E+01	$1/N^3$
Acceleration etc.	Centrifuge accel.	g	1	50	N
	Vibration accel.	g	0.15	7.5	N
	Displacement	m	50	1	1/N
	Frequency	Hz	1	50	N

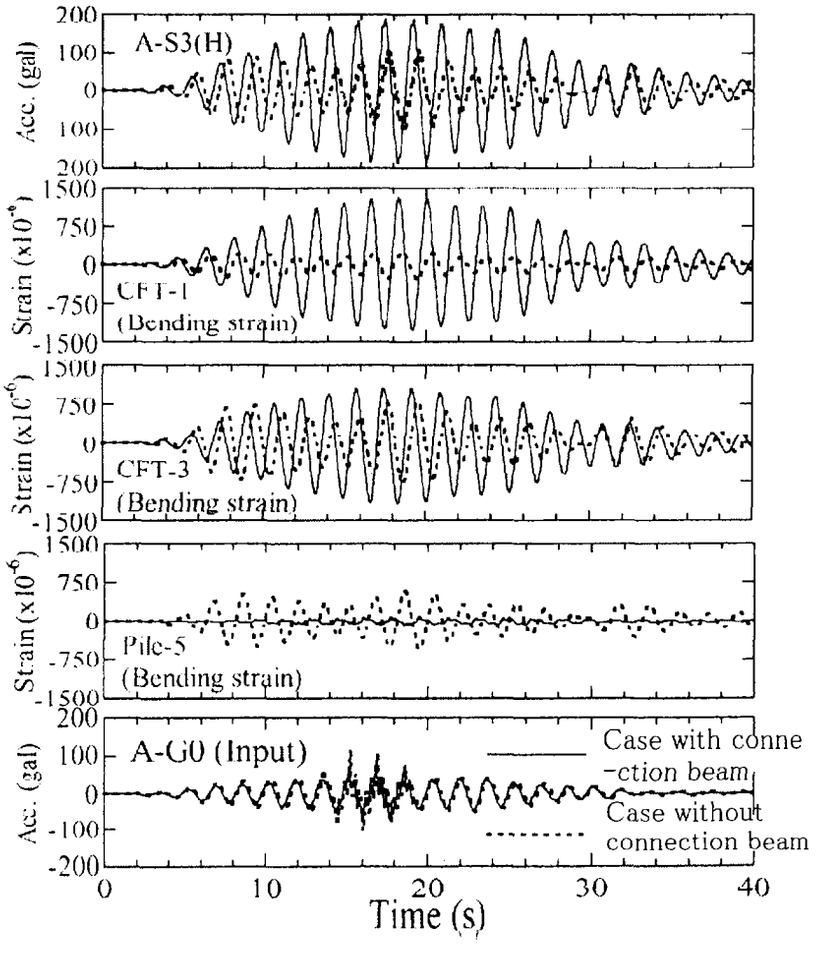

Fig. 3. Time history response of acceleration of viaduct top and bending strain of CFT pillar and pile head

Fig. 3 shows the time history response of the acceleration of the viaduct top and the bending strain of the CFT pillar and the pile

head. The figure is displayed in piles so that it may be easy to compare between the case equipped with the connection beam and the case without the connection beam. The input accelerations (*Fig.* 3d) are mostly in agreement between the case equipped with the connection beam and the case without the connection beam. However, a short cycle noise broke out at 14 – 19 seconds. This phenomenon caused the input acceleration to small a value as 50 Gals. This phenomenon is due to the limit of the vibration capability in the low frequency range of the vibration machine. The case equipped with the connection beam is lager than the case without the connection beam (*Fig.* 3a) with regard to the acceleration response of the viaduct top (A-S3). It is based on the vibration mode differing by the existence of the connection beam. The bending strain (*Fig.* 3b) of the upper part (CFT-3) of the CFT pillar is also influenced by the existence of the connection beam with regard to the magnitude of the acceleration of the viaduct top. *Fig.* 4 shows the distribution of the bending strains of the CFT pillar and the pile at the time with which these strains indicated the maximum values. You can find the following fact with *Fig.* 3 and *Fig.* 4. There are especially large differences between the case equipped with the connection beam and without the connection beam with regard to the bending strain at the lower part (CFT-1) of the CFT pillar and at the pile head (Pile-5). It can be inferred that this phenomenon was caused as follows. The position of the beam becomes a fixed condition closely in the case equipped with the connection beam. At the result, a big force is produced at the CFT pillar. As opposed to it, the behavior of the case without the connection beam is resembled in the jutting pile action subjected a lateral load. In consequence, the bending strain shows a continuous change between the CFT pillar and the pile head. It should be observed that the strain reached to 0.15% at the lower part of the CFT pillar. Although the vibration acceleration is as small as 50Gals, this phenomenon was occurred in the case equipped with the connection beam. This strain level is equivalent to the yield strain of the material. The big difference arises in the action of the viaduct by the existence of the connection beam. This big difference is because the frequency of the input wave is equivalent to the first natural frequency of the viaduct as mentioned above.

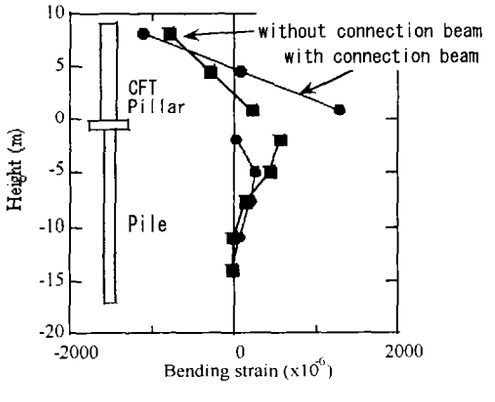

Fig. 4. Distribution of bending strains of CFT pillar and pile

Except mentioned above cases, the influence of the existence of the connection beam did not appear notably at the case of the El-Centro seismic wave and 1.0Hz Sin wave. The detail examination will be shown in the following chapter 4 by including the numerical analysis results.

NUMERICAL ANALYSIS MODEL FOR 3D-FEM

A 3-dimensional finite element analysis of the viaduct was carried out for the purpose to confirm the phenomenon that was seen in the experiment. The analysis is the equivalent linear analysis considering the time history response. *Fig.* 5 is the numerical analysis model that corresponds to the model for the dynamic centrifuge modeling. The portion of the viaduct is expressed with the beam-mass system element. The portion of the ground is expressed with the linear elastic element. In this numerical analysis, the target ground range was set up by considering the stress influence. As the boundary conditions of the lateral side of the model, the horizontal direction is free and the vertical direction is fixed. The time history wave was given as the input at the bottom of the model. This wave is equivalent to the wave that was used in the dynamic centrifuge modeling.

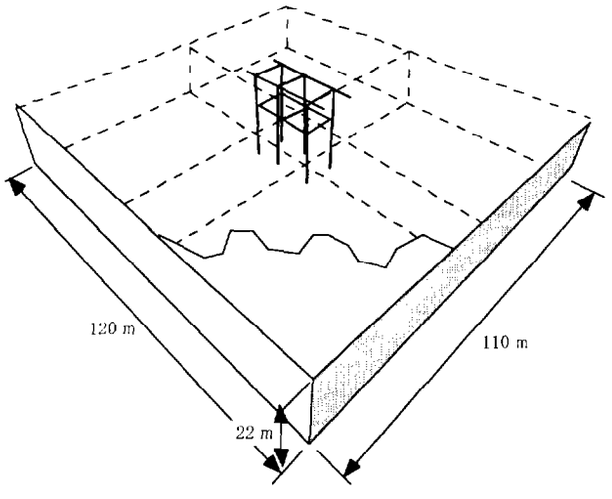

Fig. 5. Analysis model for 3-dimentional time historical finite element method

Table 2. List of parameter values of soil used for numerical analysis

Layer	Item	Adopted value
1	Young modulus	89 MN/m^2
	Poisson ratio	0.4
	Damping factor	0.15
2	Young modulus	745 MN/m^2
	Poisson ratio	0.3
	Damping factor	0.15

CHOICE OF PARAMETER VALUES OF SOIL

Table 2 is the list of the parameter values of soil used for the numerical analysis. These values were set up according to the strain level of the soil to perform the equivalent linear analysis. The concrete procedure is as follows. In the dynamic centrifuge modeling, the ground up to GL-15m was made of the silica sand and was coordinated as the relative density is equal to 70%. This situation is almost equivalent to N=16 of N-value. Then, the shear wave speed of the sandy soil can be inferred using the equation that is printed in the official design manual of the road bridge in Japan (Japan Road Society, 1990). The maximum shear modulus can be presumed as follows by using this equation.

$$V_s = 80N^{1/3} = 80 \times 16^{1/3} \cong 200\,m/s \qquad (1)$$

The modified Ramberg-Osgood model (Tatsuoka et al., 1979) is assumed as the relationship between the shear strain and the shear modulus. This assumption leads the following expression of the relations.

$$G_o = \rho V_s^2 = 0.1836 \times 200^2 = 7350\ kN/m^2 \qquad (2)$$

$$\frac{G}{G_o} = \frac{1}{1+\alpha|\gamma G|^{\beta}} \qquad (3)$$

$$\alpha = \left(\frac{2}{\gamma_{0.5}\, G_o}\right)^{\beta} \qquad (4)$$

$$\beta = \frac{2\pi h_{\max}}{2 - \pi h_{\max}} \qquad (5)$$

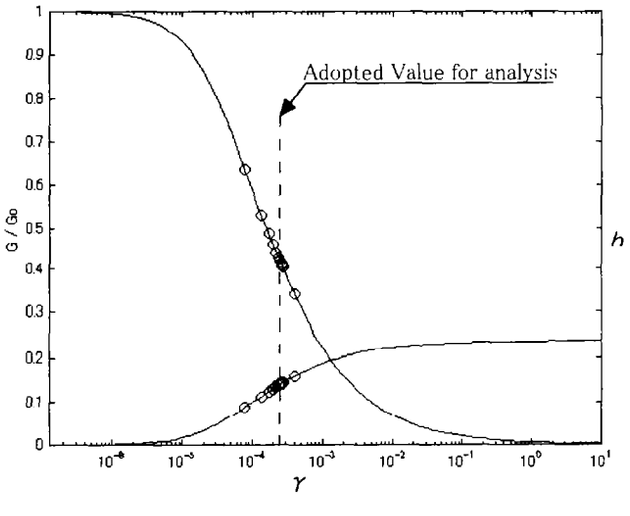

Fig. 6. Relation between the shear strain γ and shear modulus G by modified Ramberg-Osgood model

where, $\gamma_{0.5}=1.58\times10^{-4}$, $h_{max}=0.24$. *Fig.* 6 shows the relation between the shear strain γ and shear modulus G. The mark'○' is displayed on the curve of *Fig.* 6. This mark's location is obtained as follows. First, the finite element analysis for the 1-dimensional ground model was executed considering the nonlinear stress-strain relationship and the time history. At the result, the distribution of the shear strain in the ground was obtained. There, 'γ_{max}' means the maximum value of the shear strain at the each depth. The effective value of the shear strain is assumed as '0.65 γ_{max}'. The effective values of the shear strains are plotted on the X-axis of *Fig.* 6. Then, '○' marks are displayed at the position on the curve that intersect the vertical lines extended from there. The values of the shear modulus and the damping coefficients were set up as equivalent to the '○'mark of *Fig.* 6. It is presumed that these values correspond to the strain of the soil at the time of the vibration. The mean value of them is expressed by using a line in *Fig.* 6. The values of *Table* 2 are obtained in this way and are used for the analysis.

NUMERICAL ANALYSIS RESULTS

Fig. 7 and Fig. 8 were obtained by using the 0.6Hz Sin wave as the input seismic wave. Fig. 7 shows the bending moment distribution of the case equipped with the connection beam. Fig. 8 shows the bending moment distribution of the case without the connection beam. The analysis results of Fig. 7 and Fig. 8 etc. are arranged in Table 3. Table 3 is made by picking up the maximum values of the displacement and the bending moment at the each part of the structure.

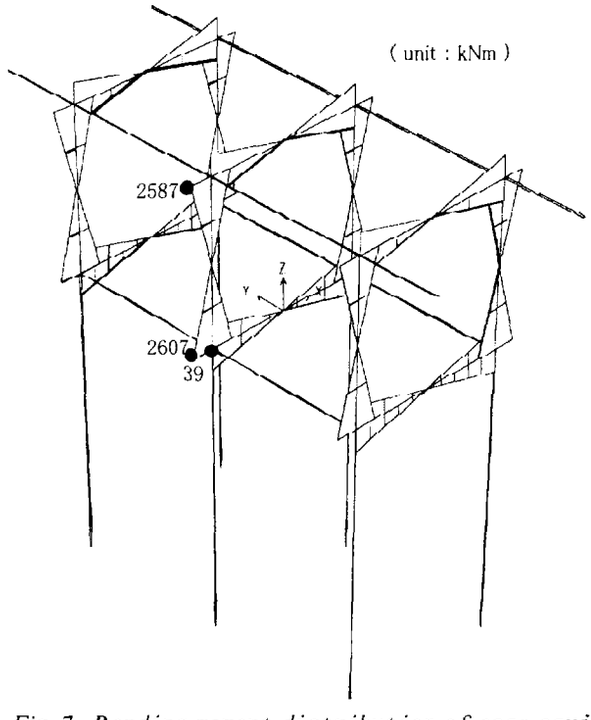

Fig. 7. Bending moment distribution of case ***equipped with connection beam*** *(Numerical analysis result that was obtained by using the 0.6Hz Sin wave as the input seismic wave)*

In *Table 3*, the numbers outside of the parenthesis are the results of the numerical analysis. The numbers inside of the parenthesis are the results of the centrifuge modeling. First, the discussion will be start from the numerical analysis results shown in *Table 3*. The case without the connection beam yields smaller values than the case equipped with the connection beam with regard to the maximum values of the lateral displacement and the moment of the pillar.

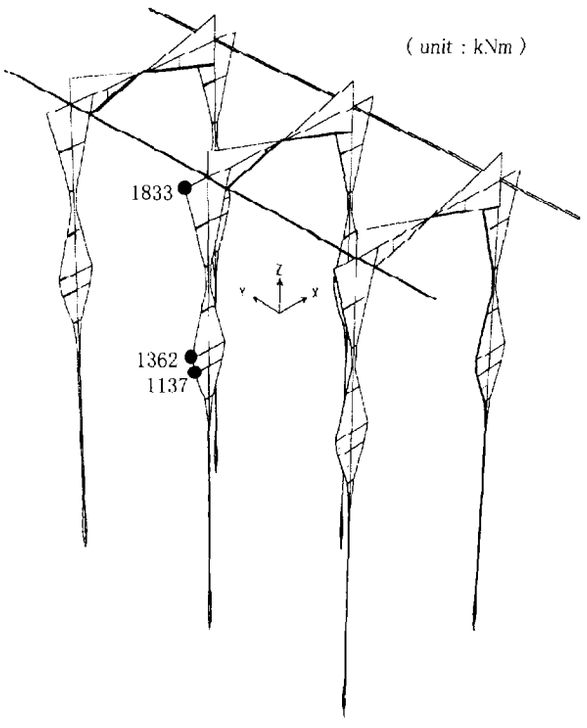

*Fig. 8. Bending moment distribution of case **without connection beam** (Numerical analysis result that was obtained by using the 0. 6Hz Sin wave as the input seismic wave)*

Table 3. Numerical analysis results and experiment results (0. 6Hz Sin input seismic wave case)

	Location	Maximum displacement (mm)	Maximum bending moment (kNm)	Axis force (kN)	First natural frequency (Hz)
Structure equipped connect-ion beam	Top of pillar	103 (150)	2587 (2450)	519	0.63
	Bottom of pillar	10	2607 (2940)	519	
	Pile head	10	39 (196)	872	
Structure without connect-ion beam	Top of pillar	99 (90)	1833 (1960)	363	0.51
	Bottom of pillar	8	1362 (588)	363	
	Pile head	8	1137 (1470)	353	

You can see the numerical analysis results coincide quantitatively and qualitatively with the experiment results in *Table* 3 for the matter. However, the case without the connection beam yields larger values than the case equipped with the connection beam with regard to the bending moment of the pile head. But, if you compare with the degree of the total stress considering the axis force, the difference is small between the two cases. It is not possible to reduce the pile diameter on a large scale, because the diameter is restricted by the other conditions (Ex. the bearing capacity). As a conclusion, it turns out that the case without the connection beam is more safety than the case equipped with the connection beam. The maximum stress and the maximum displacement are both small in the case without the connection beam. Generally speaking, this result leads a conclusion that the connection beam is not necessary for the viaduct structure. Now, the discussion will be followed by the Case using the El-Centro wave as the input seismic wave. The numerical analysis was put into practice using the El-Centro wave as the input seismic wave. *Table* 4 shows the analysis results that were arranged paying attention to the maximum values of the moment and the displacement in each part of the structure. In *Table* 4, the numbers outside of the parenthesis are the results of the numerical analysis. The numbers inside of the parenthesis are the results of the centrifuge modeling. The experiment results coincide with the numerical analysis results quantitatively and qualitatively. Namely it is guessed that numerical analysis has given the almost appropriate solution. In *Table* 4 , the case of the El-Centro seismic wave and the 0.6Hz of Sin wave are written together. According to it, the amplitude of the 0.6Hz Sin wave Case is the half of the El-Centro seismic wave's amplitude. Nevertheless, the farmer's values are 5 - 10 times of the latter's with regard to the displacement and the bending moment. As compared with the matter, the difference is small among the cases of the El-Centro seismic wave, nothing to do with the existence of the connection beam. These facts lead the following estimation. In the case of 0.6Hz Sin wave, the frequency is close to the first natural frequency of the viaduct, therefore, the influence of the existence of the connection beam is remarkable. As opposed to it, because the main frequency of the input wave is not close to the first natural frequency of the viaduct, the difference is not clear among the cases of the El-Centro seismic wave nothing to do with the existence of the connection beam.

Table 4. Numerical analysis results and experiment results (El-Centro input seismic wave case)

	Existance of beam	Location	Maximum displacement (mm)	Maximum bending moment (kNm)	Axis force (kN)	First natural frequency (Hz)
Sin wave 0.6 Hz 50 gal	Structure equipped connect-ion beam	Top of pillar	103 (150)	2587 (2450)	519	0.65
		Bottom of pillar	10	2607 (2940)	519	
		Pile head	10	39 (196)	872	
El-Centro wave 100 gal	Structure equipped connect-ion beam	Top of pillar	12 (20)	539 (490)	108	0.49
		Bottom of pillar	14	539 (490)	108	
		Pile head	14	49 (196)	176	
	Structure without connect-ion beam	Top of pillar	27 (50)	627 (980)	127	0.39
		Bottom of pillar	11	470 (343)	127	
		Pile head	11	392 (735)	118	

CONCLUSION

Generally, it is recognized that the stability of the viaduct equipped with the connection beam is higher than the viaduct without the connection beam. However, according to the results of the centrifuge modeling and the numerical analysis that were carried out this time, it was checked that this fact is not necessarily right. The results of the experiment and analysis induce the following conclusion. The structure without the connection beam is not inferior to the structure equipped with the connection beam at the viewpoint of the earthquake resistance. Especially, there is a case that the structure equipped with the connection beam causes considerably big stress and displacement. This phenomenon is caused by the frequency characteristic of the input seismic wave stands near by the first natural frequency of the viaduct. On the contrary, such a phenomenon is not seen about the structure without the connection beam. It was confirmed that the analysis results of the 3-dimensional finite element method coincide quantitatively and qualitatively with the experiment results of the dynamic centrifuge modeling.

REFERENCES

T. Shioya, K. Katuzawa, K. Dewa, T. Sato and H. Shiokawa, [1999]. Development of New Type Connection Method of CFT Pillar and RC Beam, Proc. Fourth Conf. On Recent Application of Compound, Tokyo, Japan, pp. 219-224.

Japan Road Society [1990]. Official Design Manual of Toad Bridge; Vol. of Earthquake Resistance Design, Japan.

F. Tatsuoka, T. Iwasaki, S. Fukushima and H. Sudo, [1979]. Stress Conditions and Stress Histories Affecting Shear Modulus and Damping of Sand under Cyclic Loading, Soils and Foundations, Vol. 19, No. 2., pp. 27-42.

F. Tatsuoka, T. Iwasaki, S. Yoshida, S. Fukushima and H. Sudo, [1979]. Shear Modulus and Damping by Drained Tests on Clean Sand Specimens Reconstituted by Various Methods, Soils and Foundations, Vol. 19, No. 1., pp. 39-54.